Novel Noninvasive Approach for Detecting Arteriovenous Fistula Stenosis

Hsien-Yi Wang, Cho-Han Wu, Chien-Yue Chen, and Bor-Shyh Lin*, *Member, IEEE*

***Abstract*—Hemodialysis is the most common treatment for patients with end-stage renal disease. For hemodialysis, consistently functional vascular access must be surgically created with an anastomosis of artery and vein, referred to as an arteriovenous fistula (AVF). However, AVF dysfunction may occur over time. Angiography and Doppler ultrasound are usually used to detect the flow or the diameter of the AVF. But they require well-trained operators and are expensive, and even angiography is invasive. In this study, a noninvasive approach based on stethoscope auscultation for monitoring AVF stenosis was proposed. Here, a wireless blood flow sound recorder was designed to record blood flow sounds wirelessly. In order to effectively extract the varying feature of blood flow sounds for AVF stenosis, the 2-D feature pattern built from S-transform was also proposed as the feature in the AVF stenosis detecting algorithm. Different from other frequency-related coefficients, the feature pattern can contain the information of blood flow sounds in time and frequency domains simultaneously. Preliminary findings showed that the proposed approach can provide high-quality estimation of AVF stenosis (positive predictive value = 87.84% and sensitivity = 89.24%).**

***Index Terms*—Arteriovenous fistula (AVF), blood flow sounds, hemodialysis, stethoscope auscultation, S-transform.**

I. Introduction

END-stage renal disease (ESRD), a chronic renal disease, is the progressive loss of renal function over time. For patients with ESRD, the kidneys cannot excrete the products of protein metabolism, such as urea, creatinine, etc., which results in uremic syndrome. In 2012, about 600 000 patients with ESRD underwent dialysis and renal transplantations in the United States. According to the 2012 annual report of United States renal data system (USRDS), the worldwide incidence and prevalence of patients with ESRD increases annually [1].

Manuscript received November 1, 2013; revised January 8, 2014; accepted February 24, 2014. Date of publication March 3, 2014; date of current version May 15, 2014. *Asterisk indicates corresponding author.*

H.-Yi Wang is with the Division of Nephrology, Department of Internal Medicine, Chi Mei Medical Center, Tainan 710, Taiwan (e-mail: why8@ms61.hinet.net).

C.-H. Wu is with the Institute of Imaging and Biomedical Photonics, National Chiao-Tung University, Tainan 71150, Taiwan (e-mail: s9201024@yahoo.com.tw).

C.-Y. Chen is with the Electronic Engineering, National Yunlin University of Science and Technology, Douliu 640, Taiwan (e-mail: chencyue@yuntech.edu.tw).

*B.-S. Lin is with the Institute of Imaging and Biomedical Photonics, National Chiao-Tung University, Tainan 71150, Taiwan (e-mail: borshyhlin@gmail.com).

Color versions of one or more of the figures in this paper are available online at http://ieeexplore.ieee.org.

Digital Object Identifier 10.1109/TBME.2014.2308906

The major treatments for patients with ESRD include hemodialysis, peritoneal dialysis, and renal transplantation. Until now, hemodialysis has been the most common treatment. In hemodialysis treatment, the blood is passed through a permeable membrane to quickly and efficiently remove the creatinine, urea, other waste products, and free water from the blood. For hemodialysis, a continuously functional vascular access must be surgically created with a cardiovascular anastomosis of artery and vein, referred to as an arteriovenous fistula (AVF) or arteriovenous graft [2]. The anastomosis is usually near the patient's wrist or elbow. However, the life cycle of an AVF is not long, and vascular thrombosis or stenosis may occur over time and cause the fistula to dysfunction. AVF stenosis is also a cause of the loss of performance, abnormal pressure, turbulence, or vascular calcification in hemodialysis [3], [4]. A higher percent of patients developed AVF stenosis or thrombosis [5]. Therefore, how to detect AVF stenosis early is important [6], [7].

The level of clinical vascular stenosis can be evaluated using angiography [8]. The disadvantage of angiography is that it is invasive and requires surgery. Doppler ultrasound is also used to evaluate the diameters of an AVF [9]. However, both methods and their equipment are costly and require experienced and sophisticated operators. The acoustic characteristics of AVF stenosis can also be roughly evaluated at the patient's bedside by physicians or nurses with clinical experience using stethoscope auscultation or palpation. However, up to now, most of results for stethoscope auscultation or palpation were not quantifiable.

Recently, some studies attempted to quantify and evaluate AVF stenosis by using stethoscope auscultation. In 1994, Akay *et al.* evaluated the effects of vasodilator drugs on femoral artery stenosis by using auscultation. Blood flow sounds measured from femoral artery were analyzed by using short-term Fourier (STFT) and wavelet transform (WT) methods [10]. They also indicated that isolated sounds caused by occlusions contained more energy between 200 and 800 Hz than the background sounds recorded from vessels without occlusions. In 2005, Mansy *et al.* attempted to identify acoustic parameters related to changes in vascular access patency [11]. They indicated that the blood flow sound intensity tends to increase with stenosis, and the source of this acoustic energy is associated with turbulence produced by partially occluded blood vessels. In 2006, Sato used WT analysis to investigate the relationship between shunt murmurs and assessing vascular access function [12]. Vesquez *et al.* used wavelet and empirical mode decomposition coefficients to analyze the blood flow sounds of AVF stenosis [13]–[15]. In 2011, Wang used the higher-frequency spectra (700–800 Hz) of blood flow sounds, reconstructed by WT, to detect AVF stenosis [16]. However, the frequency feature of blood flow sounds

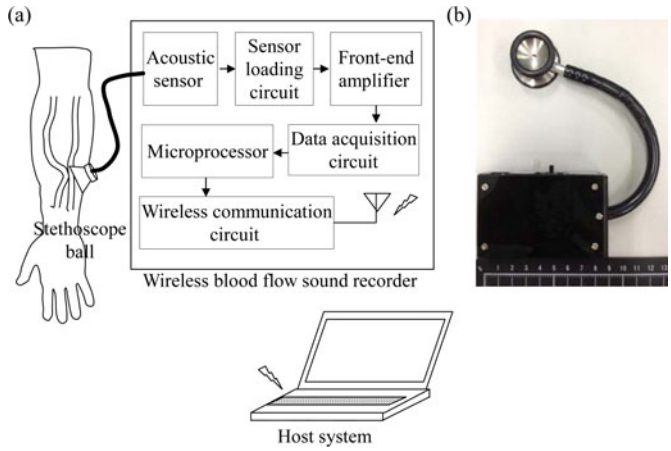

Fig. 1. (a) Basic scheme and (b) photography of proposed wireless blood flow sound recorder.

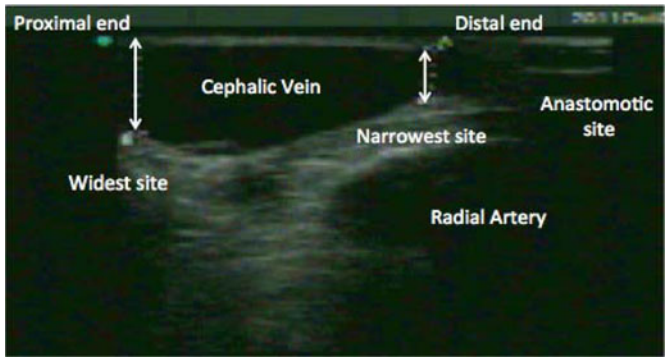

Fig. 2. Ultrasonographic illustration for definition of radiocephalic AVF stenosis. Fistula stenosis is defined as ratio of narrowest distance and adjacent widest distance is less than 50%.

related to AVF stenosis is complex due to the structure of AVF, and may be overlapped by other frequency features contributed from the friction between normal vessels and pumped flood flow during heart systole. And it may also vary with time due to the variation of blood flow rate in the cardiac cycle. Therefore, evaluating AVF stenosis by simple frequency-related coefficients may be not practicable.

In this study, a novel noninvasive approach based on stethoscope auscultation was proposed to detect AVF stenosis. Here, a 2-D feature pattern built from S-transform [17] is used as the feature in the proposed AVF stenosis detecting algorithm. The 2-D feature pattern contains the information of blood flow sounds in time and frequency domains simultaneously. Therefore, it can provide better capability of detecting the varying frequency feature of AVF stenosis than other frequency-related coefficients used in the aforementioned methods. In the proposed algorithm, radial basis function (RBF) neural network was also used to classify the feature patterns of blood flow sounds. In addition, the results of AVF stenosis examined by Doppler ultrasound were compared with the results of those examined by using the proposed method.

II. Methods

A. Wireless Blood Flow Sound Recorder

The proposed wireless sound recorder is designed to monitor and record the sound of the blood flow through an AVF. The basic scheme and photograph of the proposed recorder are shown in Fig. 1(a) and (b), respectively. The proposed recorder consists primarily of the ball of a stethoscope, an acoustic sensor, a sensor-loading circuit, a front-end amplifier circuit, a data acquisition circuit, a microprocessor, and a wireless transmission circuit. The ball of the stethoscope is used to collect blood flow sounds in the AVF. The collected blood flow sound will then be transformed into electrical signals by the acoustic sensor. The sensor-loading circuit is designed to provide a stable reference voltage to the acoustic sensor to eliminate noise caused by variations of reference voltage. The front-end amplifier circuit is a bandpass amplifier designed to amplify and filter the sound signal. After the blood flow signal has been amplified and filtered, it is digitized by the data acquisition circuit with sampling rate of 2048 Hz, which contains a sample-and-hold circuit and a 12-bit analog-to-digital converter. A microprocessor (MSP430, Texas Instruments), which contains advantages of ultralow power consumption, 16-bit reduced instruction set computing (RISC) architecture, 125-ns instruction cycle time, five power saving modes, and diversification of peripheral communication interface, controls the data acquisition circuit to obtain, preprocess, and transmit the blood flow sound data to the wireless transmission circuit, which then wirelessly transmits it to the backend host system. The wireless transmission circuit contains a printed circuit board antenna and a Bluetooth module that is fully compliant with the Bluetooth v2.0 + enhanced data rate specification. By using this Bluetooth module, it can provide sufficient transmission rate and can easily communicate with the host system built on commercial electronic devices, such as laptops and mobile phones.

B. Experiment for Detecting Fistula Stenosis

In this study, 74 participants from the division of dialysis centers at Chi Mei Medical Center, Tainan, Taiwan, were enrolled. All the patients more than 20 years old and had undergone hemodialysis three times a week for more than three months. The site of the arteriovenous surgical anastomosis was usually located near the patient's wrist or elbow on the right or left hand. Patients who had undergone major surgery or who had been hospitalized for any reason within one month before enrollment were excluded. The Institutional Review Board of Chi Mei Medical Center approved this study, and all patients signed informed consents.

A single operator performed the Doppler ultrasonography to measure the vessel diameters. An early investigation [18] reported that ultrasonic detection of significant stenosis of fistula when the ratio of the narrowest distance to the adjacent widest distance on any part of vessel is less than the 50%. Fig. 2 illustrated the definition of AVF stenosis in this study. It showed a traditional radiocephalic AVF, which was created by surgical anastomosis with radial artery and cephalic vein. Anastomotic site is near the wrist, distal to the heart. The proximal end of

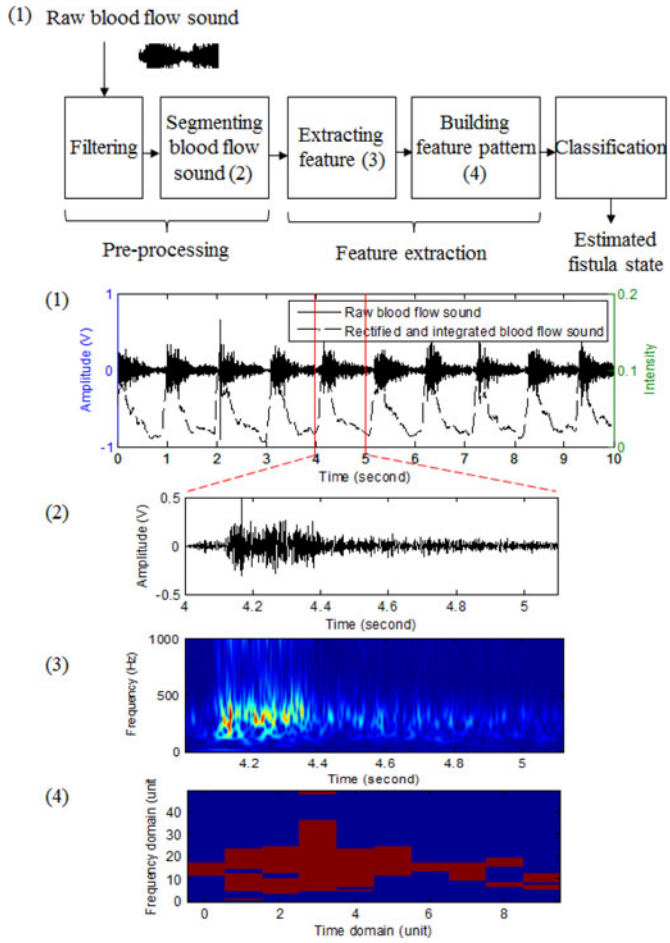

Fig. 3. Procedure of AVF stenosis detecting algorithm.

the AVF is proximal to the heart. Therefore, patients in whom the luminal diameter in the AVF was reduced $>=50\%$ were assigned to the study group, but for patients for whom this was not the case were assigned to the control group. The blood flow sound at the anastomosis of the AVF over the patient's wrist or elbow was collected using the proposed wireless blood flow sound recorder. Each sound of interest was recorded for 60 s. During this study period, the patients' treatment plans, dialysis protocol, and medications were not changed.

C. AVF Stenosis Detecting Algorithm

The pulsatile pitch of blood flow sounds through stenotic AVF are at a significantly higher frequency than that of non-stenosed AVF [10], [11], [19] and can be distinguished by experienced physicians and nurses using stethoscope auscultation. Based on these blood-flow sounds, we developed an algorithm to detect AVF stenosis, and its procedure is shown in Fig. 3. First, the raw blood flow sound is preprocessed to remove environmental noises. Next, a one-cycle blood flow sound is detected and segmented. To analyze the blood flow sound, the feature pattern of blood flow sounds in time–frequency domain is extracted by using S-transform. Finally, RBF neural network is used to classify whether or not the AVF is stenosed.

1) Preprocessing the Blood Flow Sound: Before extracting the feature pattern of blood flow sounds, the raw sound signal is preprocessed to segment the cycle of blood flow sounds. First, the raw blood flow sound is filtered using a bandpass filter with the frequency band of 100–1000 Hz to keep the meaningful features related to the state of AVF stenosis. Next, the filtered blood flow sound is rectified and integrated to obtain the envelope of the blood flow sound. The derivation of the integrated blood flow sound can then be calculated, and its peaks can be detected at the minimum value of the derivation. Finally, the cycle period of the blood flow sound can be obtained from the term between two peaks of the integrated blood flow sound.

2) Feature Extraction: After segmenting the cycle period of the blood flow sound, S-transform is used to extract the feature pattern of blood flow sounds in time–frequency domain. S-transform is a method of time–frequency analysis that uses a progressive analytic skill similar to WT to improve the performance of STFT [17]. But, different from WT, it provides precise phase information to the Fourier spectrum.

S-transform window $\omega(t)$ can be defined as a normalized Gaussian window function, and is given using the following:

$$\omega(t) = \frac{1}{\alpha\sqrt{2\pi}} e^{-\frac{t^2}{2\alpha^2}} \tag{1}$$

where t is the translation of the Gaussian function, and α is the window width, which is usually related to the frequency f of the spectral, and can be defined as $\frac{1}{|f|}$. Therefore, the S-transform value $S(\tau, f)$ of the blood flow sound $x(t)$ can be given using the following:

$$S(\tau, f) = \int_{-\infty}^{+\infty} x(t) \frac{|f|}{\sqrt{2\pi}} e^{-\frac{(\tau - t)^2 f^2}{2}} e^{-i2\pi f t} dt \tag{2}$$

where τ and f denote the time-location and the frequency of S-transform, respectively. Next, the S-transform value of a one-cycle blood flow sound in time and frequency domains is down-sampled to build a 50×10 feature pattern. Because the time interval of blood flow sound cycle may vary, the S-transform values of one-cycle blood flow sound in the time domain is equidistantly sampled at ten intervals and that in the frequency domain is also equidistantly sampled at 50 intervals to build a normalized feature pattern. Next, if the value in the feature pattern is larger than the average of the spectrum amplitude, it is set to one; otherwise, it is set to zero. Fig. 4(a) and (b) shows the time–frequency analysis using S-transform for the stenosis and non-stenosis states and for their feature patterns, respectively. By using the feature pattern built from S-transform, the varying frequency feature of AVF stenosis can be efficiently and completely reserved.

3) Classification: Radial basis function neural network is used to classify and discriminate feature patterns in this study. RBF network is usually trained to map a vector (input data) into the other vector (supervised output data), and this mapping can be viewed as a function approximation problem. It has been efficiently and successfully applied for classifications of various biomedical signals [20]. The output of the network is a linear combination of RBFs of the inputs and neuron parameters (the

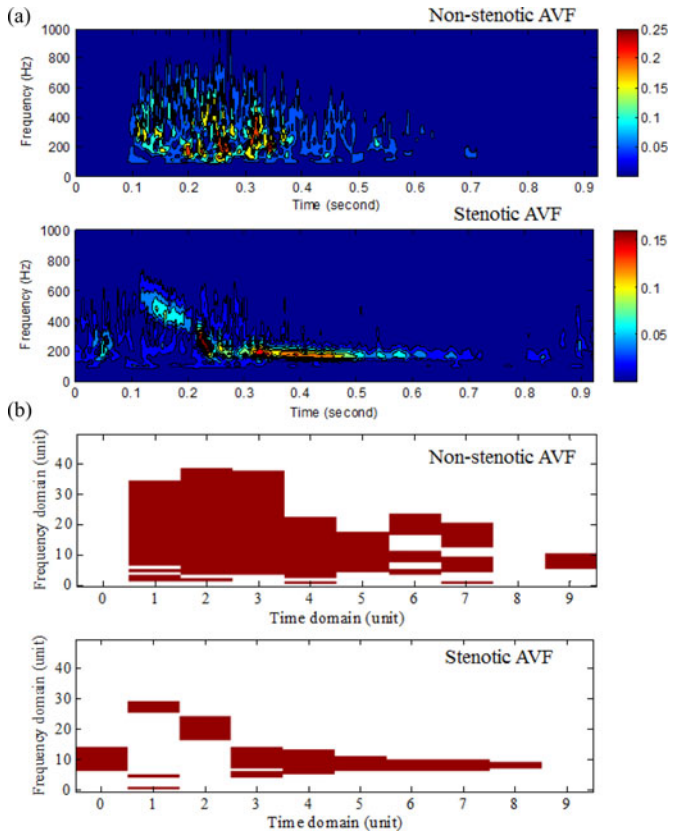

Fig. 4. (a) Time–frequency analysis by using S-transform for stenotic and non-stenotic AVF, and (b) their feature patterns.

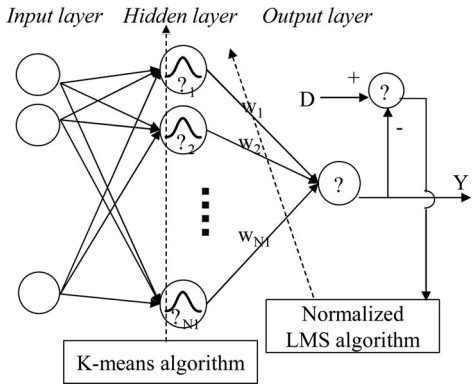

Fig. 5. Basic scheme of RBF network.

output of RBF). Therefore, it provides the advantages of extremely fast training and requirement of fewer training samples.

The basic scheme of the RBF neural network commonly contains three layers: input, hidden, and output, as shown in Fig. 5. Let N_0 and N_1 denote the number of the input layer and the hidden layer, respectively. The output Y of the RBF neural network can be calculated using the following:

$$Y = \mathbf{\Phi}^T \mathbf{W} \tag{3}$$

where $\mathbf{W} = [w_1, w_2, \ldots, w_{N_1}]^{\mathrm{T}}$ denotes the weight vector connecting the hidden and output layers, and $\mathbf{\Phi} = [\phi_1, \phi_2, \ldots, \phi_{N_1}]^{\mathrm{T}}$ denotes the node outputs in the hidden layer, generated by the Gaussian basis function. For the kth hidden node, ϕ_k can be given using the following:

$$\phi_k = \exp\left(-\frac{\|P - C_k\|^2}{2\sigma^2}\right) \tag{4}$$

where $\mathbf{P}$ denotes the feature pattern, and is used as the input of the RBF neural network. Here, σ is the estimated variance of the feature patterns, and $\mathbf{C}_k$ denotes the center matrix in the kth hidden node. $\|\bullet\|$ denotes the Euclidean norm.

In this study, the k-means clustering algorithm [21], [22], which is a self-organized learning procedure, is used for adapting the center matrices. The center matrices at the iteration t can then be adapted using the following:

$$\begin{cases} \mathbf{C}_i(t) = \mathbf{C}_i(t-1) + \mu_c[\mathbf{P} - \mathbf{C}_i(t-1)], \\ \quad \mathrm{i} = \arg\min[\|\mathbf{P} - \mathbf{C}_j(t-1)\|, 1 \le j \le N_1] \\ \mathbf{C}_k(t) = \mathbf{C}_k(t-1), \quad 1 \le k \le N_1 \text{ and } k \ne i \end{cases} \tag{5}$$

where μ_c denotes the learning rate for adapting the center matrices. The normalized least mean square algorithm is also used to adapt the weight vector W. The weight vector at the iteration t can then be adapted using the following:

$$W(t) = W(t-1) + \frac{\mu_w}{(1 + \mathbf{\Phi}^T \mathbf{\Phi})}\mathbf{\Phi}(D - Y) \tag{6}$$

where μ_w denotes the learning rate for adapting the weight vector. Here, D denotes the desired signal: 1 when the state of the AVF is stenosis; 0 when the state of the AVF is non-stenosis. Finally, the optimal threshold for discriminating the state of the AVF was found. If the output of the RBF network is larger than the optimal threshold, the estimated state of the AVF is stenosis; otherwise, if the output of the RBF network is smaller than the optimal threshold, the estimated state of the AVF is non-stenosis.

III. Results

A. Feature Extraction of Blood Flow Sound

Short-time Fourier transform and continuous wavelet transform (CWT) were used to analyze the feature of the blood-flow sounds in time–frequency domain for stenotic and non-stenotic AVF, and their results are shown in Fig. 6(a) and (b), respectively. For all of STFT, CWT, and S-transform [see Fig. 4(a)], the spectra of blood flow sounds under non-stenotic AVF significantly distributed from 200 to 600 Hz during 0.1–0.3 s. And after 0.3 s, the spectral amplitudes of blood flow sounds rapidly decayed.

Compared with the results of non-stenotic AVF cases, the spectra of blood flow sounds under stenotic AVF presented significantly narrower and higher spectral features. And the spectra of background blood flow sound, which is complex and is similar to that of non-stenotic AVF, can also be observed, but are more unapparent in this case. These narrow spectral features varied from 800 to 200 Hz during 0.1–0.3 s, and became stable at about 200 Hz after 0.3 s. Moreover, from the aforementioned results, both CWT and S-transform provided better resolution in time–frequency domain. In particular, S-transform provided more accurate phase information for the spectrum feature of AVF blood flow sound than that of CWT.

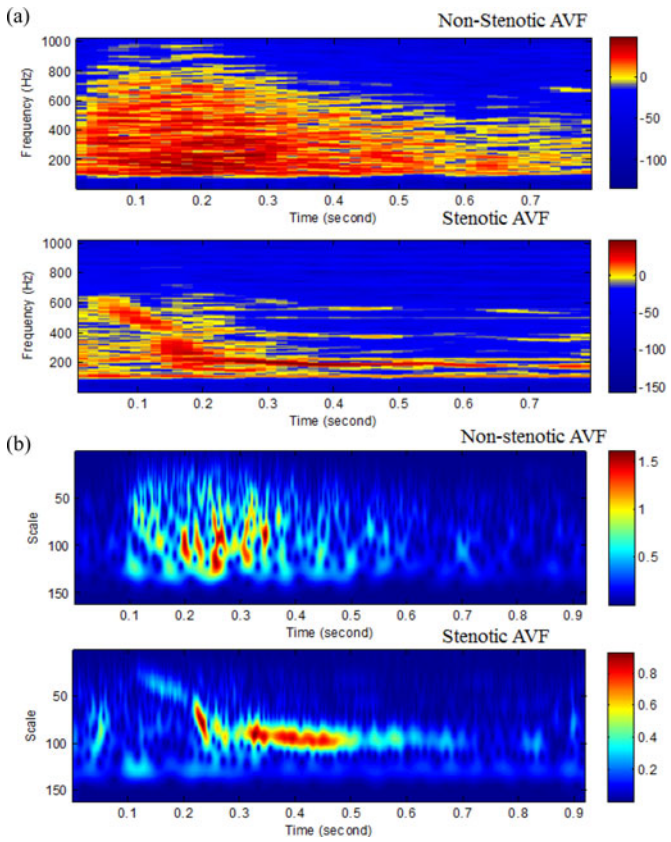

Fig. 6. Time–frequency analysis by using (a) STFT and (b) CWT for stenotic and non-stenotic AVF.

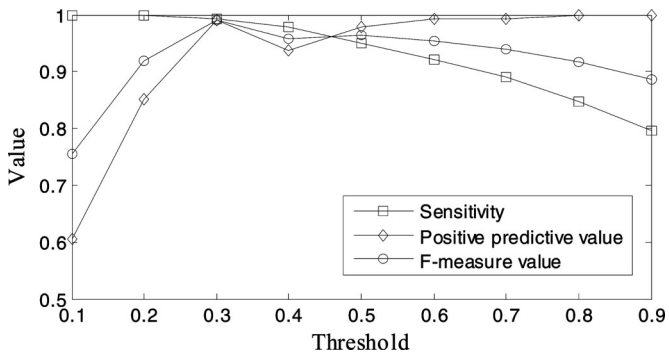

Fig. 7. Sensitivity, PPV, and F-measure value corresponding to different thresholds.

TABLE I
PERFORMANCE TEST FOR DETECTING AVF STENOSIS BY USING PROPOSED METHOD AND CWT-BASED METHOD

		Estimated result using proposed method	
		+	–
Judgement from ultrasonography	+	224 (TP)	27 (FN)
	-	31 (FP)	197 (TN)

		Estimated result using CWT-based method	
		+	–
Judgement from ultrasonography	+	213 (TP)	38 (FN)
	-	72 (FP)	156 (TN)

(TP: True-positive; FN: False-negative; FP: False-positive; TN: True-negative.)

B. Performance Evaluation of Detecting AVF Stenosis

Before evaluating the performance of detecting AVF stenosis, the optimal threshold used in the AVF stenosis-detecting algorithm has to first be determined. Here, the value of the F-measure is used to determine the optimal threshold. The F-measure is the harmonic mean of precision (positive predictive value, PPV) and recall (sensitivity); its value can be calculated using (7):

$$F = 2 \times \frac{\text{precision} \times \text{recall}}{\text{precision} + \text{recall}} \tag{7}$$

In order to calculate the PPV and sensitivity, several parameters of binary classification test were defined: True-Positive (the stenotic AVF is correctly identified as stenotic), False-Positive (the non-stenotic AVF is incorrectly identified as stenotic), True-Negative (the non-stenotic AVF is correctly identified as non-stenotic), and False-Negative (the stenotic AVF is incorrectly identified as non-stenotic). In the training phase, the numbers of the input nodes and hidden nodes in the RBF neural network were set to 500 and 16, respectively, and the range of the threshold value was set from 0.1 to 0.9. A total of 207 trials for non-stenotic AVF and 192 trials for stenotic AVF recorded in Chi Mei Medical Center dialysis center were used for training. The F-measure, PPV, and sensitivity corresponding to different threshold values are shown in Fig. 7. The value of the F-measure was distributed between about 75.41% and 98.98%, and the optimal value of the F-measure was 98.98% (PPV = 99.13% and sensitivity = 99.28%) when the threshold value was set to 0.3.

Next, the performance of detecting AVF stenosis using the proposed algorithm was evaluated. A total of 228 trials for non-stenotic AVF and 251 for stenotic AVF are used for test. The binary classification test for detecting stenotic AVF is shown in Table I. It showed the value of F-measure was 88.54% (PPV = 87.84% and sensitivity = 89.24%). The experimental result for test presented the excellent performance of the proposed method for detecting AVF stenosis.

The performance of CWT-based method for detecting AVF stenosis was also investigated. The same testing trials were used for test and the result is also shown in Table I. Here, the feature patterns were extracted by using CWT. It showed the value of F-measure was 79.48% (PPV = 74.74% and sensitivity = 84.86%). Therefore, using the feature patterns extracted by S-transform to detect AVF stenosis is exactly superior to that of CWT.

IV. DISCUSSIONS

For non-stenotic AVF, the spectra of blood flow sound are complex and are mainly distributed from 200 to 600 Hz during 0.1–0.3 s. This may be explained by that the friction between normal vessels and a great deal of pumped flood during heart systole produces a complex blood flow sound, and contributes the spectra of blood flow sounds with many different frequencies.

When the heart systole ends, the pumped blood flow rapidly reduced and this also results in the spectra amplitudes of blood flow sounds rapidly decayed after 0.3 s.

For stenotic AVF, the spectra of blood flow sounds for AVF stenosis presents significantly narrower feature at a higher frequency during 0.1–0.3 s. This significant feature is called seagull murmur, generated by turbulence in the narrow vessel [23]. During normal cardiac cycle, systolic phase with large amount of blood flow was transmitted rapidly through the arteriovenous anastomotic site with murmur and turbulence formation. The frequency of the murmurs correlated with the fistula diameter. The narrower site of fistula created higher pitch of the murmur than the wider [10]–[12]. The observed phenomenon also fits that the blood flow sound intensity at higher frequency tends to increase with stenosis. In the result of Fig. 4(a), the narrower spectral feature of AVF stenosis varied from 800 to 200 Hz after about 0.3 s. This may be explained by a great deal of pumped blood during the heart systole (0.1–0.3 s) increased turbulence at the location of AVF stenosis, and resulted in obviously higher spectral feature (about 600–800 Hz) of blood flow sound. In this case, the complex spectra of background blood flow during heart systole is still vaguely seen, but is also inhibited by the more significant feature of AVF stenosis. When the heart systole ends, the pumped blood flow reduced and this also reduced the spectral amplitude of the background blood flow sound. And the turbulence caused from the remained blood flow at the location of AVF stenosis maintains the significant spectral feature at about 200 Hz.

From the aforementioned results, S-transform provided a more accurate resolution in the time–frequency spectrum than that of STFT and CWT. STFT is one of the most commonly time–frequency analysis methods. However, its disadvantage is that, because of the limitations of its fixed window width, it cannot track the signal dynamics properly for nonstationary biosignals. S-transform uses a scalable localizing Gaussian window for dilations and translations to represent the blood-flow signal [24]. Therefore, like CWT, S-transform is excellent for extracting information from both the time and the frequency domains. However, different from the mother wavelet used in CWT, which can be separated into two parts (the slowly varying envelope that localizes in time, and the oscillatory exponential kernel that selects the frequency being localized [24]), the scalable Gaussian window used in S-transform provides more accurate phase information. Finally, both S-transform and CWT are used to extract the feature patterns of AVF stenosis. Using the feature patterns extracted by S-transform exactly provides better performance of detecting AVF stenosis than that of CWT.

Vesquez *et al*. used wavelet and empirical mode decomposition coefficients to analyze the blood flow sound, and the accuracy for detecting AVF stenosis is about 83% $\sim$ 85% [13]–[15]. Wang used the higher frequency spectra of the wavelet reconstructed blood flow sound to detect AVF stenosis, and its accuracy is also about 85% [16]. However, from our experimental results, the frequency feature of blood flow sounds related to AVF stenosis is complex, and may also vary with time due to the variation of blood flow rate in the cardiac cycle. The proposed method exactly provides better performance for detecting AVF stenosis than the aforementioned methods.

V. Conclusion

In this study, a noninvasive approach based on auscultation was proposed for monitoring the AVF function. Here, a wireless blood flow sound recorder was also designed to collect blood flow sounds wirelessly. By using the technique of S-transform, the feature pattern of blood flow sounds for the normal and stenosis states can be effectively extracted and discriminated. And from the experimental results, the proposed AVF stenosis detecting algorithm can exactly provide high efficiency for identifying the stenosis of AVF from blood flow sounds analysis.

References

[1] A. J. Collins *et al.*, "United States Renal Data System 2011 Annual Data Report: Atlas of chronic kidney disease & end-stage renal disease in the United States," *American J. Kidney Diseases*, vol. 59, pp. 1–420, 2012.

[2] M. J. Brescia, J. E. Cimino, K. Appel, and B. J. Hurwich, "Chronic hemodialysis using venipuncture and a surgically created arteriovenous fistula," *New England J. Med.*, vol. 275, pp. 1089–1092, 1966.

[3] R. L. Kirkeeide, D. F. Young, and N. R. Cholvin, "Wall vibrations induced by flow through simulated stenoses in models and arteries," *J. Biomech.*, vol. 10, pp. 431–441, 1977.

[4] J. J. Fredberg, "Origin and character of vascular murmurs: Model studies," *J. Acoustical Soc. Amer.*, vol. 61, pp. 1077–1085, 1977.

[5] D. N. Churchill, N. Muirhead, M. Goldstein, G. Posen, W. Fay, M. L. Beecroft, J. Gorman, and D. W. Taylor, "Probability of thrombosis of vascular access among hemodialysis patients treated with recombinant human erythropoietin," *J. Am. Soc. Nephrology*, vol. 4, pp. 1809–1813, 1994.

[6] D. Pagano, M. Green, M. Henderson, W. Kmiot, and M. Goldman, "Surveillance policy for early detection of failing arteriovenous fistulae for haemodialysis," *Nephrol. Dialysis Transplantation*, vol. 9, pp. 277–279, 1994.

[7] S. Sivanesan, T. V. How, and A. Bakran, "Sites of stenosis in AV fistulae for haemodialysis access," *Nephrol. Dialysis Transplantation*, vol. 14, pp. 118–120, 1999.

[8] S. Bash, J. P. Villablanca, R. Jahan, G. Duckwiler, M. Tillis, C. Kidwell, J. Saver, and J. Sayre, "Intracranial vascular stenosis and occlusive disease: evaluation with CT angiography, MR angiography, and digital subtraction angiography," *Amer. J. Neuroradiol.*, vol. 26, pp. 1012–1021, 2005.

[9] N. Tessitore, V. Bedogna, L. Gammaro, G. Lipari, A. Poli, E. Baggio, M. Firpo, G. Morana, G. Mansueto, and G. Maschio, "Diagnostic accuracy of ultrasound dilution access blood flow measurement in detecting stenosis and predicting thrombosis in native forearm arteriovenous fistulae for hemodialysis," *Amer. J. Kidney Diseases*, vol. 42, pp. 331–341, 2003.

[10] M. Akay, Y. M. Akay, W. Welkowitz, and S. Lewkowicz, "Investigating the effects of vasodilator drugs on the turbulent sound caused by femoral artery stenosis using short-term Fourier and wavelet transform methods," *IEEE Trans. Biomed. Eng.*, vol. 41, no. 10, pp. 921–928, Oct. 1994.

[11] H. A. Mansy, S. J. Hoxie, N. H. Patel, and R. H. Sandler, "Computerised analysis of auscultatory sounds associated with vascular patency of haemodialysis access," *Med. Biolog. Eng. Comput.*, vol. 43, pp. 56–62, 2005.

[12] T. Sato, K. Tsuji, N. Kawashima, T. Agishi, and H. Toma, "Evaluation of blood access dysfunction based on a wavelet transform analysis of shunt murmurs," *J. Artif. Organs*, vol. 9, pp. 97–104, 2006.

[13] P. Vesquez, M. M. Marco, and B. Mandersson, "Arteriovenous fistula stenosis detection using wavelets and support vector machines," in *Proc. IEEE Eng. Med. Biol. Soc. Conf.*, 2009, pp. 1298–1301.

[14] P. Vasquez, M. M. Marco, E. Mattsson, and B. Mandersson, "Application of the empirical mode decomposition in the study of murmurs from arteriovenous fistula stenosis," in *Proc. IEEE Eng. Med. Biol. Soc. Conf.*, 2010, pp. 947–950.

[15] M. M. Munguía and B. Mandersson, "Analysis of the vascular sounds of the arteriovenous fistula's anastomosis," in *Proc. Proc. IEEE Eng. Med. Biol. Soc. Conf.*, 2011, pp. 3784–3787.

[16] Y.-N. Wang, C.-Y. Chan, and S.-J. Chou, "The detection of arteriovenous fistula stenosis for hemodialysis based on wavelet transform," *Int. J. Adv. Comput. Sci.*, vol. 1, pp. 16–22, 2011.
[17] R. G. Stockwell, L. Mansinha, and R. P. Lowe, "Localization of the complex spectrum: The S transform," *IEEE Trans. Signal Process.*, vol. 44, no. 4, pp. 998–1001, Apr. 1996.
[18] A. Asif, F. N. Gadalean, D. Merrill, G. Cherla, C. D. Cipleu, D. L. Epstein, and D. Roth, "Inflow stenosis in arteriovenous fistulas and grafts: A multicenter, prospective study," *Kidney Int.*, vol. 67, pp. 1986–1992, 2005.
[19] J. Z. Wang, B. Tie, W. Welkowitz, J. L. Semmlow, and J. B. Kostis, "Modeling sound generation in stenosed coronary arteries," *IEEE Trans. Biomed. Eng.*, vol. 37, no. 11, pp. 1087–1094, Nov. 1990.
[20] M. Akay, *"Nonlinear Biomedical Signal Processing: Fuzzy Logic, Neural Networks, and New Algorithms*. vol. 1. New York, NY, USA: Wiley-IEEE Press, 2000.
[21] C. Sheng, B. Mulgrew, and P. M. Grant, "A clustering technique for digital communications channel equalization using radial basis function networks," *IEEE Trans. Neural Netw.*, vol. 4, no. 4, pp. 570–590, Jul. 1993.
[22] J. C. Bezdek, *Pattern Recognition With Fuzzy Objective Function Algorithms*. Norwell, MA, USA: Kluwer Academic Publishers, 1981.
[23] C. S. Hayek, W. R. Thompson, C. Tuchinda, R. A. Wojcik, and J. S. Lombardo, "Wavelet processing of systolic murmurs to assist with clinical diagnosis of heart disease," *Biomed. Instrum. Technol.*, vol. 37, pp. 263–270, 2003.
[24] S. Ventosa, C. Simon, M. Schimmel, J. J. Danobeitia, and A. Manuel, "The S-transform from a wavelet point of view," *IEEE Trans. Signal Process.*, vol. 56, pp. 2771–2780, 2008.

Hsien-Yi Wang received the B.S. degree from Taipei Medical University, Taipei, Taiwan, in 1995 and the M.S. degree in executive master of business administration from National Cheng Kung University, Tainan, Taiwan, in 2013.

He is currently an Assistant Professor of the Department of Sport Management, Chia Nan University of Pharmacy, Tainan and a Physician of Division of Nephrology, Chi Mei Medical Center, Tainan. His research interests include the areas of biological fluid proteomics, dialysis, and chronic kidney diseases.

Cho-Han Wu received the B.S. degree in electrical engineering from Fu Jen Catholic University, Taipei, Taiwan, in 2010, and the M.S. degree from the Institute of Imaging and Biomedical Photonics, National Chiao Tung University, Hsinchu, Taiwan, in 2013.

His current research interests include biomedical signal processing.

Chien-Yue Chen received the B.S. degree in physics from Soochow University, Taipei, Taiwan, in 1992, the M.S. and Ph.D. degrees in space science and optical science individually, both from National Central University in 1994 and 2004, respectively.

He is currently a Professor at the Department of Electronics Engineering, National Yunlin University of Science and Technology, Douliu, Taiwan.

Bor-Shyh Lin (M'02) received the B.S. degree from National Chiao Tung University (NCTU), Hsinchu, Taiwan, in 1997, the M.S. and Ph.D. degrees in electrical engineering from National Taiwan University (NTU), Taipei, Taiwan, in 1999 and 2006, respectively.

He is currently an Associate Professor of the Institute of Imaging and Biomedical Photonics, NCTU, Taiwan. His research interests include the areas of biomedical circuits and systems, biomedical signal processing, and biosensor.